

MEMOIRE DE STAGE DE MASTER 2e ANNEE

effectué à l'Institut des Géosciences de l'environnement
Sous la direction 'Charles Amory' and 'Kevin Fourteau'



Évolution de la neige en période de fonte : modélisation et observation au Col du Lautaret

par

Glenn Pitiot



OpenReproLab

This research internship benefited from the support of the laboratory's digital platform, as part of the OpenReproLab initiative. The students had access to a cloud-based computing environment. They also took part in weekly training sessions focused on coding practices and data management aimed at improving the reproducibility of results. These trainings, along with support throughout the internship from members of the digital platform, introduced tools, methods, and a work organization that promote direct integration of the project into the methodologies and best practices to deliver open and reproducible science.

Plein de mercis mercis mercis mercis mercis mercis mercis mercis mercis mercis mercis mercis mercis mercis à

À mes deux encadrants Kévin et Charles. Je n'aurais pas pu avoir un meilleur encadrement.

Laurent, qui m'a enseigné l'utilisation de tous les appareils de mesure et qui a toujours été de bon conseil pour le développement et le déploiement des CS655.

Hélène et Catherine, dont l'aide technique, tant en amont de la campagne que pendant, a permis de réaliser cette campagne de mesures.

Toute l'équipe de support du Jardin du Lautaret, notamment Pascal et Lucie, qui nous ont aidés durant toute la campagne, et sans qui elle n'aurait pas été aussi poussée.

Toutes celles et ceux qui nous ont aidés directement dans la campagne en participant à des jours de mesures, comme Arnaud, Giulia, Benjamin et Philippe.

Marie et Neige, qui m'ont permis de participer à cette chouette expérience qu'est la Snow School.

Sarah et Didier, qui m'ont aidé avec les données météorologiques.

Toute l'équipe d'OpenReproLab, qui m'a fourni des outils et une rigueur de travail qui guideront mes futurs travaux.

Mathieu et Audrey, qui m'ont aidé à installer CROCUS.

À Gislain, qui m'a aiguillé de temps à autre, mais toujours dans la bonne direction.

À Matthieu Lafaysse qui a accepté de prendre de son temps pour être le rapporteur de ce stage. Je lui souhaite une bonne lecture.

Abstracts

The ongoing development of snow models requires the study of wet and melting snowpacks. Identifying the key mechanisms at play for water percolation within a natural snowpack is thus critical to model this complex process. To that end, I participated in the set-up of an field campaign during the melting season 2024–2025 at Col du Lautaret in the Alps. Its goal is to provide a clearer picture of water flow in a natural snowpack and to foster instrumental development. The deployment of continuous temperature and liquid water content measurements, alongside snow pit profiles carried out during the melt period, was used to study the percolation dynamics. It was further used to analyze the performance of two percolation schemes, the bucket scheme and Richards equation, in the detailed snowpack model Crocus. The Richards percolation scheme theoretically allows a better modelling of the complexity of percolation compared to the Bucket scheme, an idealized representation of percolation, but is more computationally costly. Unfortunately, results show that the commercial liquid water sensors selected for this internship are inadequate for snow monitoring. The rest of field observations suggest the important role of capillary barriers and refreezing crusts in influencing the water percolation dynamics. However, the Richards scheme did not provide a better representation of these barriers compared to the Bucket scheme, raising questions about the benefit of a more complex scheme. It appears that a key missing mechanism in our modelling attempt is percolation along preferential paths, leading to a poor representation of the temperature profiles in Crocus for both schemes. Further development are thus two folds : developing measurements able to continuously measure liquid water content in snow, and tailoring numerical schemes to capture the dominant mechanisms at play during percolation.

Améliorer la modélisation de la neige nécessite l'étude de son humidification. Identifier les paramètres clés de la percolation de l'eau liquide dans le manteau neigeux devient dès lors un véritable enjeu. Dans ce cadre, j'ai participé à une campagne de mesures innovante au col du Lautaret, dans les Alpes, durant la saison 2024–2025. Des mesures continues de température et de teneur en eau liquide, couplées à des profils issus de puits à neige, ont été déployées afin d'étudier la dynamique de la percolation. Ces données ont permis de tester deux schémas de percolation dans CROCUS, un modèle détaillé du manteau neigeux. Le schéma basé sur les équations de Richards permet, en théorie, une représentation plus fine de la percolation, mais s'avère plus coûteux en calcul que le schéma Bucket, qui en propose une version plus idéalisée.

Malheureusement, le capteur sélectionné pour mesurer la teneur en eau liquide ne semble pas adapté à une utilisation dans la neige. Néanmoins, le reste de la campagne a permis d'identifier, les barrières capillaires et les couches de regel, comme des facteurs majeurs influençant la percolation. Cependant, tout comme le schéma Bucket, le schéma Richards n'a pas permis une meilleure représentation de ces phénomènes, remettant en question la plus-value apportée par une telle complexité. L'absence de représentation des chemins préférentiels de percolation dans les deux schémas conduit à une modélisation erronée des profils de température. Les développements futurs devront donc s'orienter vers : le développement d'une technique de mesure continue de la teneur en eau liquide dans la neige et l'implémentation des mécanismes majeurs de la percolation dans les modèles, notamment les flux préférentiels

Contents

OpenReproLab	3
Abstracts	1
Contents	3
List of Figures	5
Introduction	7
1 Methods and experimental protocol for the evaluation of percolation schemes	9
1 Time Domain Reflectometry for continuous measurement of liquid water content	9
1.1 Experimental techniques to measure liquid water in snow	9
1.2 Theory behind Time Domain Reflectometry	10
1.3 Comparison between Campbell TDR CS655 and WISe sensors from cold room experiments	11
2 Field Campaign During the 2025 Melt Season at Col du Lautaret	12
2.1 FluxAlp meteorological station	12
2.2 Autonomous snow observations	13
2.3 Manual snow pit observations	13
3 Crocus Simulation	15
3.1 What is Crocus	15
3.2 Forcing meteorological data.	15
3.3 Bucket and Richards: two different ways of representing liquid water percolation	16
3.4 Simulation settings and objectives	17
2 Experimental and simulation results	19
1 Time domain reflectometry for liquid water content measurement	19
1.1 Comparison of CS655 and WISe sensors: Can the CS655 match WISe measurements?	19
2 Observing the dynamics of liquid water percolation and refreezing within a natural snowpack during the 2025 Melt Season at Col du Lautaret	20
2.1 A brief note on the CS655 sensors in the field	20
2.2 Diurnal cycle observations	21
2.3 Can refreezing crusts, capillary barriers, and SSA be linked?	22
3 Added-value of Richards' equation over a simple bucket scheme and comparison with observations	22
3.1 Overall differences in the snowpack melting behaviour	23
3.2 Assessing the performance of the Bucket and Richards percolation schemes against observations of the temperature profile	24

3	Discussion and perspectives	27
1	Prospects for future development of liquid water content measurements	27
2	Designing the next field campaign	28
2.1	Feedbacks of the campaign	28
2.2	Next steps to enhance wet snow investigations on the field	28
3	Retrospective and future directions in the development of water percola- tion schemes	29
3.1	Analyzing the settings simulations used	29
3.2	Considerations on the future development of percolation schemes	30
	Conclusion	33
	Bibliography	35
A	Method for forcing files creation	39
1	Gap filling	39
2	Precipitation treatment	39
B	Detailed description of Bucket and Richards percolation scheme	43
1	Modelling liquid water percolation in snow: the bucket scheme	43
2	Modelling liquid water percolation in snow: Richards equations	43

List of Figures

1.1	Schematic representation of Time Domain Reflectometry operation	10
1.2	Experimental setup for cold room comparison between Time Domain Reflectometry CS655 and WISe sensors	11
1.3	Localisation of FLuxAlp station at Col du Lautaret	12
1.4	Instruments During Melt Season 2025: ASSSAP (SSA), WISe (LWC), Snow Cutter (Density) — TDR & PT100 for Continuous Snowpack Monitoring	14
1.5	Schematic of the response of three snowpacks to a water input. The first and second ones use Bucket, and differ only in the first layer. The third one uses Richards percolation scheme. Due to higher density, Snowpack 1 has a 1.6 greater water holding capacity in the top layer than Snowpack 2, allowing it to retain more water and delay percolation and runoff. Richards allows a dynamics representation of the percolation.	16
2.1	Comparison between the CS655 TDR and WISe sensors, using two techniques for computing the permittivity for the CS655: from an empirical formula directly provided by the sensor ("Campbell" dots), or from fundamental electromagnetic laws. Liquid water content is then calculated using Eq. 1.1 with density of 350 kg/m^3	20
2.2	Diurnal Cycle Observations : Observations of totla density, LWC, and SSA at Col du Lautaret during the 2024–2025 melting season. The right pannem shows a picture of upper part of the snowpack, with the identified refreezing crust.	21
2.3	ASSSAP Specific Surface Area (SSA) Profiles at Col du Lautaret (08/04/2025) – Three temporally separated profiles from nearby locations, and a stratigraphy from a snow pit near the SSA profile at 11:00 am (not representative of SSA data)	23
2.4	Density and LWC simulated using the Crocus model with the Bucket (BKT) and Richards (RCH) percolation schemes	24
2.5	Temperature simulated using the Crocus model with the BKT and RCH percolation schemes and observed temperatures (OBS) measured by PT100 sensors. The observations are spatially interpolated between each sensor. Snow depth is scaled from the ground (0 cm) to 142 cm, which corresponds to the position of the uppermost PT100 sensor.	25
A.1	Schematic of the relative topography of the FluxAlp station to explain over- and under-accumulation snow events.	40
A.2	Observed snow depth (black) at Col du Lautaret from SnowView vs. Crocus-simulated snow depth forced with various precipitation inputs: "Obs precip" uses SnowView-observed precipitation; "CRO precip 3h no Smooth" and "CRO precip 24h no Smooth" use reconstructed precipitation from snow depth using the Crocus density formula over 3h and 24h intervals	41

B.1	Schematic Van Genuchten Model With and Without Cutoff (Right/Left)	. 44
-----	--	------

Introduction

Scientific context

Snow is a key component of the global climate system. It continuously covers glaciers and ice sheets, and seasonally covers nearly one-third of the Earth's land surface (Sturm et Liston, 2021). Snow regulates surface energy exchanges with its high albedo and low thermal conductivity. It acts as the primary source of mass for ice sheets and glacier, influencing sea level and representing a freshwater resource downstream of many mountain regions (Viviroli et al., 2007). However, observations show a gradual decline in both the extent and duration of seasonal snow cover, indicating earlier snow melt onset (Bormann et al., 2018). Meltwater is also increasingly observed on ice sheets where it contributes to mass loss either directly through runoff or indirectly via interactions with ice dynamics (Amory et al., 2024). In this context, liquid water is emerging as a central driver of snowpack evolution and surface energy and water budgets at the planetary scale.

Understanding the behavior of liquid water within snow requires a detailed view of snow physical properties and their evolution. Snow is a dynamic porous medium composed of ice grains and air, whose microstructure (defined as the size, shape, and arrangement of grains and bonds) evolves with time under the action of humidity, temperature and pressure gradients, a process known as metamorphism. The percolation of liquid water depends on this microstructure and, in turn, water alters it by refreezing and warming the snowpack. Meltwater also influences albedo through metamorphism, affecting the energy balance of the snow and, consequently, the rate of melt. These interdependent processes give the snowpack a "memory," where present conditions are shaped by past events, complicating its representation in models. For example, capillary barriers (i.e., interfaces between two porous layers of contrasting pore sizes, visible as horizontal layers filled with colored water in the picture on the front page of this report) can delay or block percolation, causing water to accumulate above the interface. Refreezing at these locations can form ice crusts, reducing local porosity and affecting water retention capacity. Such complexities underscore the challenges involved in modelling snow-water interactions (Verjans et al., 2019).

Snow models incorporate water percolation processes using approaches of varying complexity. The Crocus model, developed at the Centre d'Études de la Neige (CEN), simulates snowpack evolution in detail and recently integrated the Richards formalism (Richards, 1931) as a physically-based alternative to the widely used "bucket" scheme (D'Amboise et al., 2017). In the bucket approach, snow layers are treated as reservoirs with fixed water retention capacity and excess water is passed downward. While the Richards-based approach provides a more physically detailed representation of water percolation based on the snowpack's physical properties, it remains computationally intensive and has yet to be fully evaluated. Regardless of their complexity, all these modeling approaches require detailed field observations to assess their ability to accurately represent water content, pathways, and infiltration depth (Wever et al., 2015).

Objectives and research questions

This internship aims to evaluate different representations of water percolation in snow using field observations from an alpine site. The work is structured around two main objectives: (1) building a dataset for evaluating percolation schemes, and (2) applying

this dataset to the Crocus model. By comparing simulations with field data, the study seeks to identify key processes and assess the benefits of using more physically detailed approaches. Ultimately, this work aims to address the following research questions:

i) How to measure liquid water content into the snow? The challenge lies in achieving measurements that are qualitative (detecting the presence or absence of liquid water), quantitative (estimating the liquid water content), continuous (autonomous over time), and vertically resolved (to capture water content gradients and infiltration depth).

ii) What are the differences and performance characteristics of the Bucket and Richards percolation schemes for water flow in snow?

This report is structured as follows: Chapter 1 describes the methods used to measure liquid water content, the fieldwork carried out during the 2024–2025 melt season, and the scenarios applied in the Crocus simulations. Chapter 2 presents the main results. Chapter 3 discusses these findings and outlines proposed future developments for studying water percolation. To support quick and efficient reading, the report includes Key Notes at the beginning of Chapter 1 and 2 and alongside each main result in Chapter 2, highlighting the most important information.

Methods and experimental protocol for the evaluation of percolation schemes

In this chapter, I describe a method for continuously measuring liquid water content in wet snow, which has been more commonly been applied to wet soils. I also present an innovative measurement campaign designed to support snowpack modeling studies. Finally, I outline the modeling choices made using the Crocus snow model, with the goal of comparing two different water percolation schemes.

1 Time Domain Reflectometry for continuous measurement of liquid water content

Key Notes : *The snow dielectric permittivity highly depends on the presence of water. TDR sensors use electromagnetic waves to measure the dielectric permittivity in order to access the liquid water content.*

1.1 Experimental techniques to measure liquid water in snow

Measuring the liquid water content (LWC) continuously in snowpacks remains an open experimental challenge. Several techniques have been developed to estimate the presence of liquid water and its percolation through the snowpack (e.g., [Quéno et al., 2020](#); [Samimi et al., 2021](#); [Priestley et al., 2022](#)). However, no reference method currently exists for continuously monitoring the LWC profile throughout an entire season.

One such technique is the Self-Potential method. This passive approach measures the electrical potential generated by water flow within the snowpack. It was recently deployed at Col de Porte ([Priestley et al., 2022](#)) and shows promise for studying the timing of percolation. However, it does not provide direct access to LWC values.

Radar techniques can detect both the timing of percolation and estimate LWC ([Heilig et al., 2018](#)). Nevertheless, this method requires specialized expertise¹, which is currently not available in Grenoble.

Finally, the Time Domain Reflectometry (TDR) method offers a viable option for continuously monitoring LWC in snowpacks, making it a valuable tool for long-term snow hydrology studies ([Samimi et al., 2021](#); [Madore et al., 2022](#)). The Campbell CS655² TDR is chosen because it can provide a continuous, discrete and autonomous measurement of LWC at relatively low cost. Although widely used in soil studies, this sensor has only rarely been applied to snow, and results regarding its performance, both from qualitative

¹Raw radar data must be interpreted using inverse models to derive the LWC.

²CS655 sensor: <https://www.campbellsci.fr/cs655>

(detect the presence of liquid water) and quantitative (estimate the liquid water content) perspectives have been mixed (Samimi *et al.*, 2021; Clerx *et al.*, 2022).

1.2 Theory behind Time Domain Reflectometry

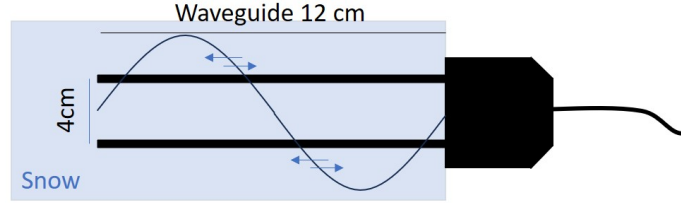


Figure 1.1: Schematic representation of Time Domain Reflectometry operation

TDR measures the relative dielectric permittivity ϵ (dimensionless) of a medium. In the case of snow, ϵ can be used to estimate the LWC. Indeed, snow is composed of ice ($\epsilon_{\text{ice}} = 3.2$)³, air ($\epsilon_{\text{air}} = 1$), and liquid water ($\epsilon_{\text{water}} = 81$). The bulk permittivity of a porous medium is an average of those of its components (which holds for long wavelegnths only). Thus, the presence of liquid water significantly increases the bulk permittivity of snow. Typically, bulk permittivity ranges from about 2 for dry snow to 4 for wet snow. Two main approaches are commonly used to relate ϵ to the LWC. The first approach involves using an idealized dielectric mixing model, such as the one proposed by Birchak *et al.* (1974). The second approach relies on experimental relationships. For example, the WISe sensor uses an empirical formula derived from measurements by Denoth (1989), shown in Equation 1.1. To ensure consistency between sensors, the empirical formula from Denoth and Ambach has been used in this internship⁴:

$$\epsilon = 1 + 1.202(D - D_w) + 0.983(D - D_w)^2 + 21.3D_w \quad (1.1)$$

Where:

- D is the total snow density [g/cm^3]
- D_w is the liquid water density in snow [g/cm^3]

$\text{LWC}_{\text{Vol}} = \frac{D_w}{\rho_v} \times 100$ (%) (with $\rho_v = 1\text{g}/\text{cm}^3$ the intrinsic density of liquid water) represents the percentage of snow volume occupied by liquid water.

To measure the permittivity, a TDR sensor sends an electromagnetic wave along a waveguide (Fig. 1.1), that is reflected at its open-end. This wave is slowed down depending on the permittivity of the medium. Thus, by measuring the travel time of the wave,

³Note that permittivity values are illustrative; actual values depend on temperature and frequency

⁴Campbell CS655 provides an other empirical relationship, but derived for soils

one can estimate the permittivity of the medium around it. Thus, the permittivity ϵ is calculated using:

$$\epsilon = \left(\frac{tc_0}{d} \right)^2 \quad (1.2)$$

With :

- $d = 2L$, and $L = 12$ cm is the length of the CS655 waveguide.
- C_0 is the velocity of light in vacuum.
- t is the time of flight between the emission and the reception.

The CS655 sensor provides direct data processing using empirical formulas specific to the sensor in order to determine the permittivity. However, since no detailed information is available on these formulas, two values of permittivity were exploited in this internship. The first is computed using Equation 1.2 and the time of flight provided by the CS655 sensor. The second is the permittivity value post-processed and directly given by the CS655 sensor.

1.3 Comparison between Campbell TDR CS655 and WISe sensors from cold room experiments

I carried out tests to assess the accuracy and validity of the CS655 sensor compared to the WISe sensor (see Section 2.3). The experimental protocol was simply to measure the permittivity of snow with varying moisture content using both sensors and to compare the readings.

In the experimental setup (Figure 1.2), one CS655 probe was inserted into a snow stack inside a cool box, with the upper face exposed to warm air. Simultaneously, three WISe measurements were taken to minimize uncertainty due to spatial variability. The process was repeated at different moisture levels, with the snow being homogenized and reformed between tests to ensure consistent conditions.

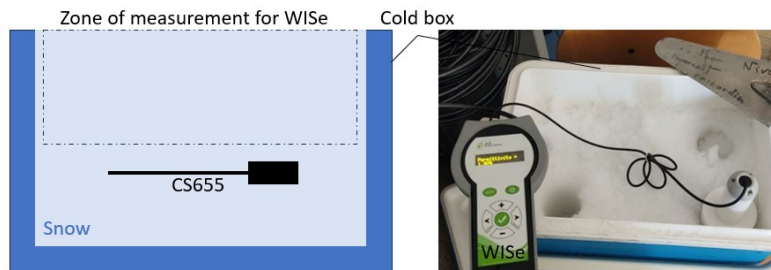


Figure 1.2: Experimental setup for cold room comparison between Time Domain Reflectometry CS655 and WISe sensors

2 Field Campaign During the 2025 Melt Season at Col du Lautaret

Key Notes : *During the melting season 2024–2025 at Col du Lautaret, several instruments were deployed to study wet snow. Digging snow pits allowed the measurement of snow stratigraphy, as well as density, liquid water content and specific surface area profiles during some interesting melting days. Temperature and liquid water content were also measured continuously using PT100 and CS655 sensors.*

The Col du Lautaret ($45^{\circ}02'28.7''$ N, $6^{\circ}24'38.0''$ E; 2100 m a.s.l.) is a particularly valuable site for snow observations in alpine conditions, owing to its elevation and topographic setting, which support the accumulation of a seasonal snowpack reaching several meters in depth before spring melt begins. Continuous snow measurements combined with ad hoc measurements in snow pits were performed to create a database for snow modelling evaluation, with a focus on the water percolation process. Another asset of this location is that the meteorological station FluxAlp is established there.

2.1 FluxAlp meteorological station

Col du Lautaret has hosted the [FluxAlp](#) meteorological station since 2016, which aims at documenting energy and mass fluxes in the soil-snow-vegetation-atmosphere continuum of an alpine catchment. The station continuously records a variety of meteorological variables, necessary to understand the snowpack dynamics and to model it. Combined with the technical infrastructure provided by the Jardin du Lautaret, this logistical and technical support was essential for the collection of valuable observation data at regular intervals along the melting season.



Figure 1.3: Localisation of FLuxAlp station at Col du Lautaret

2.2 Autonomous snow observations

To continuously monitor the melting of the snowpack and the associated liquid water percolation, autonomous measurements of temperature and permittivity were deployed in the snowpack at the FluxAlp site. Indeed, temperature is a key parameter to characterize the thermodynamical state of snow. In particular, the presence of liquid water can be inferred when snow reaches the fusion temperature. Thus, continuous temperature monitoring is a convenient tool, alongside permittivity measurements, to detect when melting occurs and as well as to estimate the progression of the wetting front. For this campaign, eleven PT100 and TDR sensors were installed at 10-centimeter intervals on a transparent polycarbonate structure specifically designed for this purpose at IGE. The structure was then buried vertically in the snow to span the entire depth of the snowpack (as displayed in Figure 1.4). Data were sampled every 10 seconds and stored as 5-min averages. This provided high-resolution temperature and relative permittivity profiles during the melting season. The measurements were recorded between March 17 and April 8, 2025

2.3 Manual snow pit observations

Manual snow pit profiles were conducted on March 17, 21, 31, April 1, 2, and 8, to complement the autonomous measurements with point-scale observations of snow physical properties representative of the snowpack state at the time of measurement.

Density measurements

Snow density is a key microstructural property, moreover required for the conversion of permittivity measurements into LWC estimates. It ranges from 100 kg/m^3 for fresh snow to around 400 kg/m^3 for compacted snow. A snow sample of known volume $V = 146.5 \text{ cm}^3$ is collected with a snow cutter (Figure 1.4) and weighted. Then, density is calculated as the mass-to-volume ratio. Typical resolution for snow density profiles was 5 cm with a snow cutter thickness of 2 cm. Unfortunately, this does not allow to measure small density variations, such as those induced by refreezing crusts.

SSA measurements

The Specific Surface Area (SSA) defined as the surface area per unit mass of ice is another key parameter for studying the microstructure of snow. It reflects both the complexity and the grain size of snow, and is currently the most effective metric for analysing microstructural changes such as metamorphism. SSA ranges of value are from $5 \text{ m}^2/\text{kg}$ for old, wet snow to $50\text{--}70 \text{ m}^2/\text{kg}$ for fresh, dry snow. The ASSSAP (Autonomous Snow Specific Surface Area Profiler) sensor (Arnaud *et al.*, 2011) allows to measure either a snow sample or vertical profiles at high resolution (cm). Both reflected irradiance from a laser diode (1030 nm) and distance of the sample are measured and converted into SSA.



Figure 1.4: Instruments During Melt Season 2025: ASSAP (SSA), WISe (LWC), Snow Cutter (Density) — TDR & PT100 for Continuous Snowpack Monitoring

Liquid water content measurements

The Liquid Water Content (LWC) is defined as the percentage of liquid water volume relative to the total volume of a snow sample. LWC typically ranges from 0% in dry snow to approximately 10% in wet snow. The WISe sensor measures the dielectric permittivity of the snow, which, when combined with density measurements, can be used to estimate LWC, similarly to TDR techniques.

The measurement principle relies on creating an electromagnetic resonance within a cavity (the cylindrical body of the WISe sensor), which imposes a fixed frequency. Since the frequency and wavelength of the wave are related through the dielectric permittivity, it is possible to infer the permittivity of the snow by comparison with a reference medium, such as air.

The main source of uncertainty in these measurements arises from probe insertion. Over-compaction of snow inside the cavity can lead to an overestimation of permittivity, while the presence of air pockets results in an underestimation. Despite this, the WISe sensor has proven to be highly robust over time. Both laboratory and field tests confirm good repeatability, with variations of less than 5% between consecutive measurements.

3 Crocus Simulation

Key Notes : *A short simulation beginning on the 17-03-2025 and forced with Flux-Alp data was used for the comparison of two percolation schemes. The Bucket scheme is an idealized representation of percolation with low computational complexity, whereas the Richards scheme is more computationally expensive but provides a richer representation of water dynamics, including capillary barriers. Nevertheless, it has not yet been proven that increasing this complexity allows to better represent percolation dynamics in snow.*

3.1 What is Crocus

Crocus is the detailed snowpack model developed in Centre d'Etude de la Neige. Crocus is notably used as a support tool for avalanche forecasting—while not the primary input for bulletin preparation, it plays a key role in estimating the timing of snowpack wetting, which is critical for assessing wet-snow avalanche risk. Improving our understanding of snowpack wetting could therefore have real value for forecasting. But as a general snowpack model, Crocus applications range beyond the estimation of avalanche risk. For instance, it is also used at the regional and global scale, in hydrological ([Vionnet et al., 2019](#)) or climatological applications ([Brun et al., 2013](#); [Royer et al., 2021](#)). To facilitate its use in such cases, Crocus has been integrated within the SURFEX land surface scheme, which notable includes a representation of the underlying soil and the interactions with it. Crocus is an Eulerian–Lagrangian model⁵ that can simulate snowpack from the onset until its melt. Briefly, at each timestep (Figure n°2 of [Vionnet et al., 2012](#)), it starts by adding a new fresh layer in case of snowfall, then compute snow metamorphism and densification, and finally solves the energy balance and liquid water percolation, taking phase changes into account. This internship focuses on the percolation scheme.

3.2 Forcing meteorological data.

The forcing file is a crucial part for running a Crocus simulation. It provides the model with the amount of precipitation and the energetic fluxes driving the surface energy balance. For my simulations, I used the FluxAlp meteorological data. To that end, gap filling was performed by interpolation using Sarah Vermaut's method (another M2 student at UGA). I paid a particular attention to reproduce precipitations consistently with the observed snow depth throughout the season. A detailed description of this procedure can be found in Appendix A.

⁵Lagrangian because the snowpack layer size is not fixed, and Eulerian because some variables, such as liquid water, move through the layers.

3.3 Bucket and Richards: two different ways of representing liquid water percolation

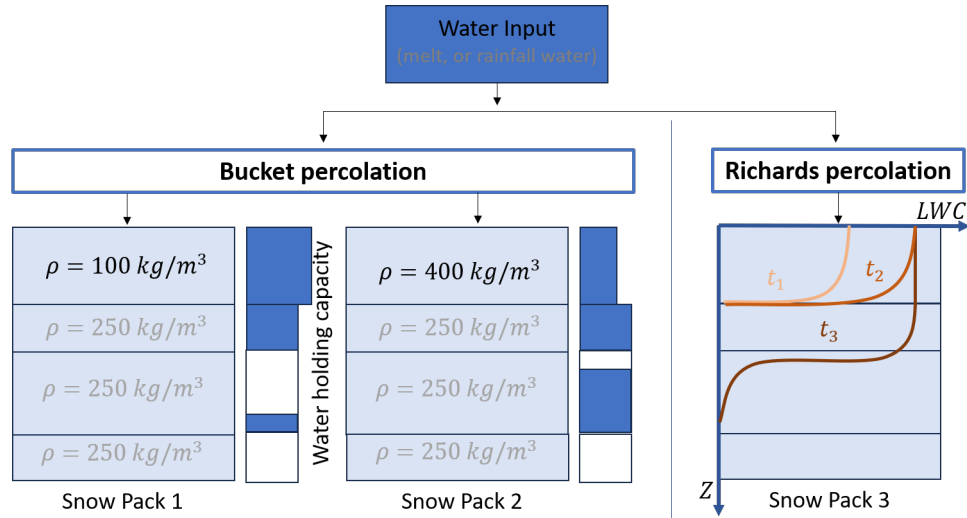


Figure 1.5: Schematic of the response of three snowpacks to a water input. The first and second ones use Bucket, and differ only in the first layer. The third one uses Richards percolation scheme. Due to higher density, Snowpack 1 has a 1.6 greater water holding capacity in the top layer than Snowpack 2, allowing it to retain more water and delay percolation and runoff. Richards allows a dynamics representation of the percolation.

As schematized in Figure 1.5, the Bucket percolation scheme (BKT) is an idealized representation of percolation with low computational complexity, whereas the Richards percolation scheme (RCH) is more computationally expensive but provides a richer representation of water dynamics.

For instance, RCH should in principle be able to represent capillary barriers forming at the interface between two layers in the snowpack. These barriers block water percolation due to the capillarity forces that are stronger in fine-grain layers than in coarse-grain layers. RCH also allows to represent percolation as a dynamic process depending of hydraulic conductivity, whereas the percolation is an instantaneous process in BKT. While Richards' equation is more physically detailed and capable of representing such processes, it requires solving a nonlinear partial differential equation, which increases computational cost. Although computation time is not a major concern for the point-wise simulations performed in this internship, it can become a significant limitation for snow schemes implemented in distributed models, such as global climate models. Despite the promising features of the RCH scheme, it has not yet been proven that its higher degree of complexity yields a better representation of percolation dynamics. Finally, it is important to note that the sequential treatment of liquid water percolation and refreezing is handled differently in the two approaches. BKT simultaneously percolates and refreezes the water layer-by-layer whereas RCH percolates water into the whole snowpack and then refreezes after.

A more detailed description of the BKT and RCH scheme can be found in the Appendix [B](#).

3.4 Simulation settings and objectives

To quantify the added-value of the RCH scheme over the standard BKT scheme, a series of simulations was conducted over several days starting on 17 March 2025, i.e. during the melt period. Focusing on a short-time interval allows a layer-by-layer comparison between the two schemes. This would not be feasible with a full-season simulation, since Crocus merges layers over time and the RCH and BKT simulations thus do not have corresponding layerings at the end of the season. In addition, observed temperature profiles can be used as an indicator of percolation dynamics. The initial conditions (temperature, density, SSA, etc) for this simulation setup are based on snowpit observations. They were directly introduced in the so-called "prep file" of Crocus to be used as the initial state of the snowpack.

Experimental and simulation results

This chapter presents the major results of my internship. Each time, the result is first described before being interpreted. First, I question the capacity of the CS655 TDR sensor to continuously measure LWC in snow. Then, I highlight key mechanisms for water percolation based on field observations during the 2025 melt season at Col du Lautaret. Finally, I analyze the behavior of both percolation schemes, RCH and BKT, in Crocus, and evaluate them against observations.

1 Time domain reflectometry for liquid water content measurement

1.1 Comparison of CS655 and WISe sensors: Can the CS655 match WISe measurements?

Key Notes : *The CS655 TDR sensor is not capable of accurately capturing the permittivity range relevant for snowpack evolution. This is likely due to the fact that snow, even in an advanced state of melt, typically exhibits much lower permittivity values than wet soils.*

Figure 2.1 presents the comparison between CS655 TDR sensor (initially developed for soil) and the WISe sensor (developed specifically for LWC measurements in snow), taken as a reference. As explained above, there are two ways to derive a permittivity value using the CS655 sensor. The permittivity value using the physical principle of electromagnetic wave travel time, referred to as "Basic laws of magnetics" (BLM) and plotted in blue in the left pannel of the figure. On the other hand, the permittivity directly given by the CS655 sensor, referred to as "Campbell" and based on an empirical law, is plotted in orange.

The BLM method does not appear to be sufficiently sensitive to increases in LWC, whereas the Campbell permittivity method seems more responsive to changes in permittivity. However, regardless of the method used, the CS655 sensor consistently underestimates permittivity. During field measurements, the wave travel time recorded by the CS655 decreased as the sensor was inserted into the snow, indicating that a physical issue may underlie these measurement discrepancies. That said, the Campbell permittivity cannot be fully trusted either, as all permittivity values above unity seem to be fixed to one. This underestimation of permittivity directly leads to an underestimation of LWC. In some cases, the LWC measured by TDR is clamped to zero to avoid reporting negative values, even though the WISe system reports soaked snow with an LWC of about 6%. This discrepancy is likely due to the permittivity values of snow being too low for the CS655 to detect reliably. Originally designed for soils (with $\varepsilon_{\text{soil}} = [7; 25]$), the CS655 is not capable of detecting small variations in snow permittivity, which typically ranges

from approximately 2.0 to 3.5. While the CS655 may capture high moisture content in snow to some extent, a significant bias between WISe and CS655 sensors leads to notable discrepancies in LWC estimation.

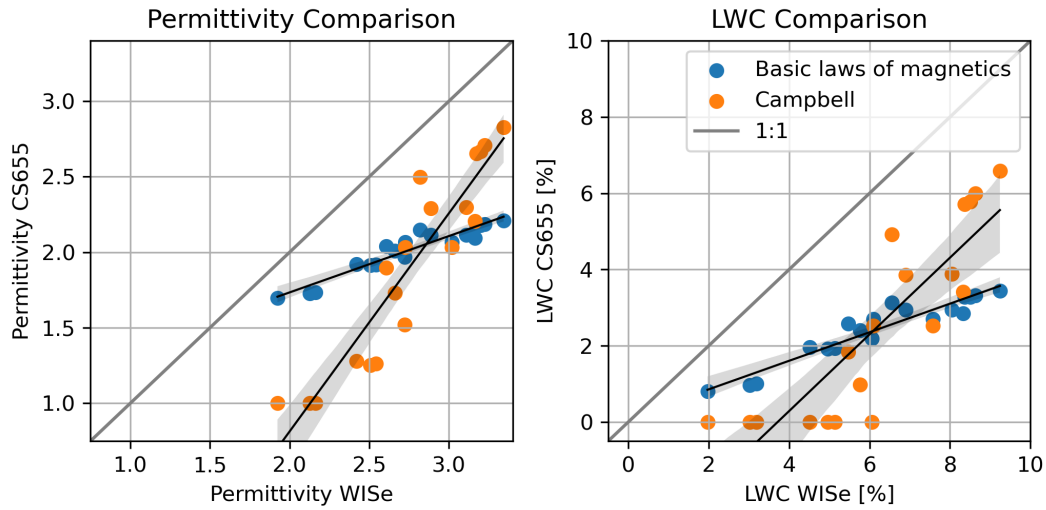


Figure 2.1: Comparison between the CS655 TDR and WISe sensors, using two techniques for computing the permittivity for the CS655: from an empirical formula directly provided by the sensor ("Campbell" dots), or from fundamental electromagnetic laws. Liquid water content is then calculated using Eq. 1.1 with density of 350 kg/m^3 .

2 Observing the dynamics of liquid water percolation and refreezing within a natural snowpack during the 2025 Melt Season at Col du Lautaret

2.1 A brief note on the CS655 sensors in the field

The array of CS655 sensors was deployed in the field before reaching my final conclusion on their inadequacy to estimate the permittivity, and hence LWC, of snow. The data collected during the melting period at Col du Lautaret were nonetheless analyzed. The estimated permittivity values are quite low (less than 1.1), whereas WISe measurements performed in the vicinity yielded permittivities of about 2.4. This is consistent with the strong negative bias observed in the cold room. Therefore, I was unfortunately unable to use the CS655 data, neither quantitatively, nor qualitatively.

2.2 Diurnal cycle observations

Key Notes : *Observations during the melt season showed a diurnal cycle of melting during the day followed by refreezing at night. During melt periods, water appeared to accumulate above an identifiable refreezing crust. No significant contrast in density nor specific surface area were observed that could explain this retention, highlighting the crucial role of refreezing crusts in influencing the percolation process.*

Figure 2.2 presents snow pit observations (total density, LWC, and SSA) from two consecutive fieldwork days, on the 31/03 and 01/04. March 31st was clearly a melting day, due to the warm and sunny meteorological conditions. As a result, the upper snow layers between 1.30 m and 1.57 m became soaked, with an LWC ranging between 5% and 10% (second pannel) and an associated increase in density. However, the rest of the snowpack remained quite dry. The next day was a colder day, without as much melting, and the snowpack was overall drier. Finally, SSA appears to remain stable during these two days, eventhough its high spatial variability makes point wise comparison delicate.

Melting water was clearly stored above 130 cm during the 31/03. However, no significant differences in SSA between this layer and the layer below seems to explain the presence of a capillary barrier (i.e., a fine-grained layer underlying a coarse-grained one). Density remains constant as well, and thus could not explain the water retention at a 10% LWC level. However, a well-defined refreezing crust separates these layers. It suggests that the refreezing crust is the reason for the water retention and thus plays a major role in controlling water percolation dynamics.

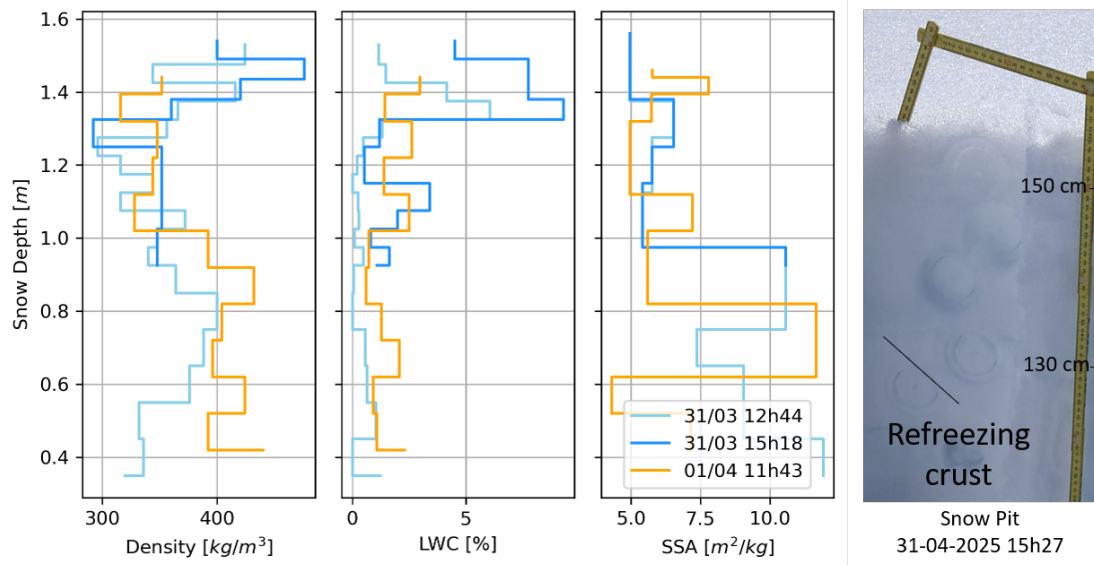


Figure 2.2: Diurnal Cycle Observations : Observations of totla density, LWC, and SSA at Col du Lautaret during the 2024–2025 melting season. The right pannem shows a picture of upper part of the snowpack, with the identified refreezing crust.

2.3 Can refreezing crusts, capillary barriers, and SSA be linked?

Key Notes : *The refreezing crusts, which might be linked to capillary barriers, do not show a significant difference in specific surface area that would indicate the formation of such a barrier. Observations appear to have been made too late to capture the key characteristics involved in the formation of the capillary barrier.*

The formation of the refreezing crust might be due to the presence of a capillary barrier, which retains liquid water above it. However, the refreezing crusts observed at Col du Lautaret do not show significant differences in specific surface area (measured with ASSSAP) that could explain the formation of such a barrier. Results are presented in Figure 2.3. A qualitative stratigraphic analysis allowed the identification of several layers characterized by observable grain size and sometimes with refreezing crusts between them. However, each time a refreezing crust was identified, it appears to be surrounded by a local decrease in SSA, rather than a fine-grain over large-grain stratigraphy.

Thus, none of the observed refreezing crusts can be associated with clearly identifiable capillary barriers. This may be either because crusts are not caused by capillary barriers, leaving their origin uncertain, or because water accumulation at the barrier level destroys the fine-grained snow that initially formed them.

A potential limit of the data collected during field days at Col du Lautaret is that the snow pit stratigraphy was not measured at the exact same location as the ASSSAP profile. As a result, the snow pits stratigraphy does not perfectly match the ASSSAP profile due to differences in snow depth and potentially in local stratigraphy. Moreover, a continuous and quantitative measurement of the LWC would have likely provided a clearer picture of the formation and evolution of capillary barriers and refreezing crusts starting from a dry snowpack. However, because of the limitation of the CS655 sensors, this study had to rely on snapshot observations performed during the melting period. It lacks information on the dry snowpack just prior to melting, which is necessary to determine the origin of the capillary barrier.

3 Added-value of Richards' equation over a simple bucket scheme and comparison with observations

The final part of this internship was dedicated to an analysis of the BKT and RCH schemes in the numerical snow model Crocus. For that, two simulations of the melting season at Col du Lautaret were performed. They use the BKT and RCH percolation schemes and were run from 17-03-2025 until the end of the melt season. In order to make the link with the field observations, I rely on the simulated and measured layer temperatures, as the CS655 data were unusable.

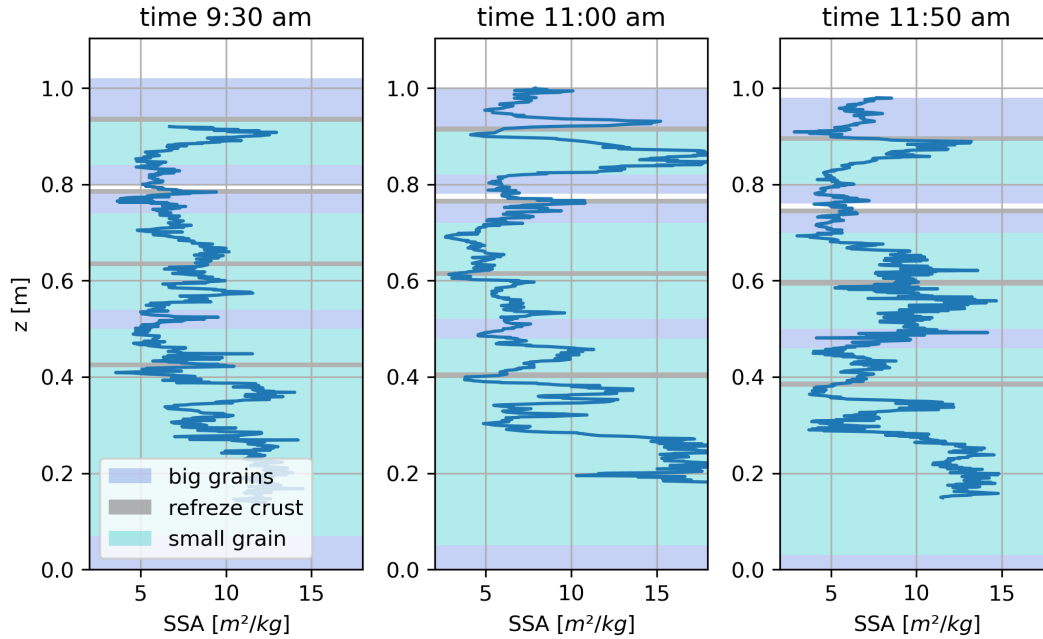


Figure 2.3: ASSSAP Specific Surface Area (SSA) Profiles at Col du Lautaret (08/04/2025) – Three temporally separated profiles from nearby locations, and a stratigraphy from a snow pit near the SSA profile at 11:00 am (not representative of SSA data)

3.1 Overall differences in the snowpack melting behaviour

Key Notes : *The Richards percolation scheme leads to earlier snowpack melting compared to the Bucket scheme at Col du Lautaret. This is likely due to the sequential treatment of percolation and refreezing, which is handled differently in the two approaches.*

The comparison between the RCH and BKT simulations highlights a different wetting dynamics depending on the percolation scheme used (Figure 2.4).

The overall wetting of the snowpack occurs more rapidly in BKT, in which a wetting front percolates from the surface to the base within a few days. In contrast, in RCH, the wetting process is slower, but the basal layers of the snowpack become soaked before the wetting front has fully progressed through the entire snowpack. Another notable difference between the two schemes is that diurnal cycles are simulated in RCH, with daily spikes of the LWC percolating downward, and not in BKT. Finally, a striking feature is that snowmelt is generally much faster with RCH than with BKT. In the case of the Col du Lautaret simulation, this leads to a total snowpack melt days occurring a couple of weeks earlier than in the RCH scheme. Observations of the density profile in Figure 2.4 show that in fact, in the RCH scheme, melting tends to occur at the bottom of the snowpack, where individual layers of similar density appear to collapse at the bottom. Conversely, BKT only melts layer by layer from the top to the bottom.

Since the markedly greater melting in the RCH case represents a significant difference from the BKT scheme, it is important to investigate its cause and evaluate its physical plausibility. My understanding is that it is due to the sequential treatment of the percolation and refreezing in the RCH scheme. Indeed, snow can be seen as gravel-like material, where percolation is fast and the RCH representation quickly allows water to go through the entire snowpack. In RCH, small quantities of water flows through the entire snowpack without refreezing at the beginning of the melting season, it then warms the bottom part which is already close to the melting point, and leads to the presence of LWC at the bottom. On the other hand, liquid water in the cold middle of the snowpack refreezes after the percolation step and is thus not visible in the right pannel of Figure 2.4. This warming of the bottom may favor its melting, consequently leading to earlier melt for RCH compared to BKT.

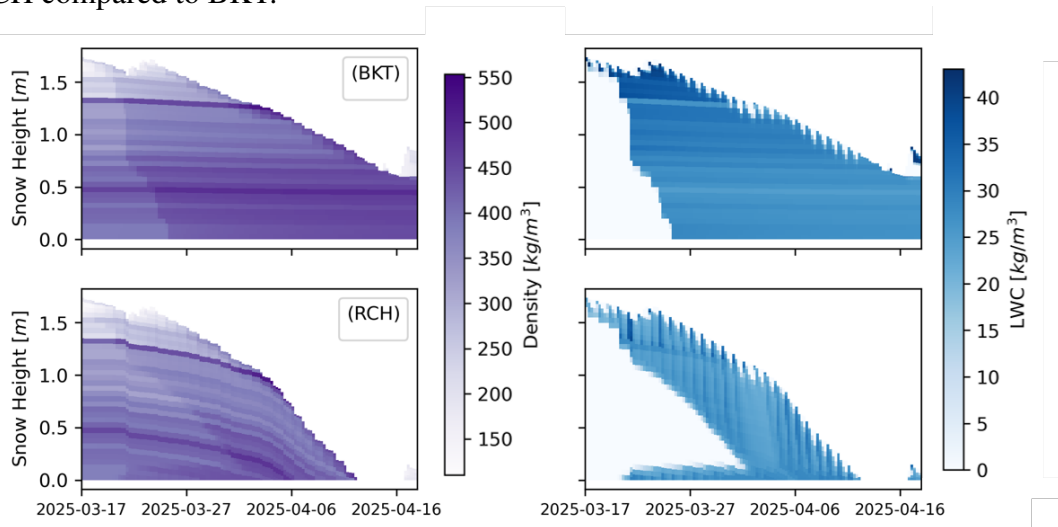


Figure 2.4: Density and LWC simulated using the Crocus model with the Bucket (BKT) and Richards (RCH) percolation schemes

3.2 Assessing the performance of the Bucket and Richards percolation schemes against observations of the temperature profile

Key Notes : *Temperature observations show that both the Bucket and Richards schemes fail to capture the warming of a deep snowpack layer likely caused by preferential water flow. This highlights the benefit to explicitly represent preferential flow in percolation schemes. A clear capillary barrier was identified in the observations but was not reproduced in the simulations, raising questions about both the ability of the Richards and Bucket scheme to simulate such features and the role of the model's initial conditions.*

The temperature observations strongly suggest that water percolated along preferential

path ¹, a process not represented by neither RCH nor BKT (Figure 2.5).

The wetting front appears earlier in observations than in BKT and RCH. Moreover, observations show warming of the snowpack from both the bottom and the top. Conversely, warming in BKT and RCH comes only from the top.

Temperature observations reveal the presence of a warm spot at about 1m height. This position corresponds to the refreezing crust discussed in Section 2. This is consistent with the idea that a capillary barrier retained liquid water at that location, and that refreezing of this liquid water lead to both the crust and a warm point due to the release of latent heat. However, both models (RCH and BKT) appears unlikely to reproduce such mechanism.

This brings attention to the role of preferential flow. As a result, liquid water can percolate directly to the bottom of the snowpack without significantly warming intermediate layers. Only matrix flow is implemented in BKT and RCH, preventing the representation of such processes. The heat accumulation near 1 m likely marks the position of a capillary barrier, raising questions about the ability of BKT and RCH to capture capillary barriers, as well as the accuracy of the initial profiles used in the simulations.

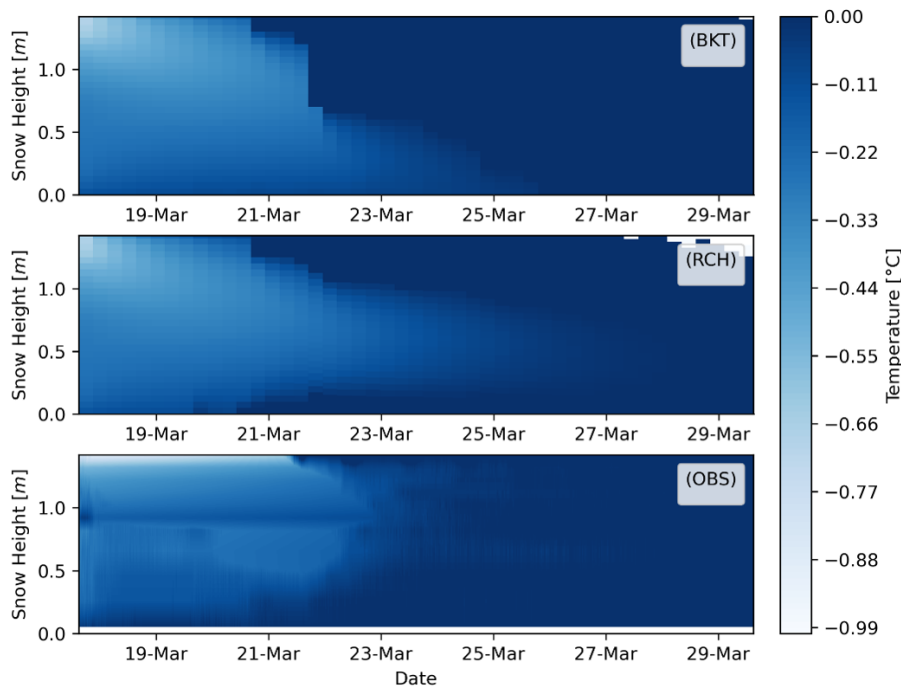


Figure 2.5: Temperature simulated using the Crocus model with the BKT and RCH percolation schemes and observed temperatures (OBS) measured by PT100 sensors. The observations are spatially interpolated between each sensor. Snow depth is scaled from the ground (0 cm) to 142 cm, which corresponds to the position of the uppermost PT100 sensor.

¹Flow of water into the snow can be divided into two: matrix flow, taking place throughout the whole microstructure, and preferential flow, taking place chimneys and allowing water to percolate rapidly without refreezing.

Discussion and perspectives

Key Notes : *Since temperature profiles alone cannot capture the post-thermalization dynamics of the snowpack, accessing raw TDR data and exploring variations in waveguide geometry appear to be promising avenues for estimating the liquid water content in snow. A detailed analysis of the snowpack in dry conditions prior to melt is also essential to identify the key structural parameters driving the formation of capillary barriers. Furthermore, the melt–albedo feedback could be better understood by examining the influence of liquid water on the spectral albedo. In addition, targeted experiments are needed to determine whether refreezing or percolation occurs more rapidly during melt onset, which is critical for the development of physically consistent numerical models. Finally, the representation of preferential flow does not necessarily require the full complexity of a Richards-based formulation; intermediate-complexity approaches may offer a more computationally efficient alternative while still capturing the dominant processes.*

1 Prospects for future development of liquid water content measurements

The CS655 TDR sensor is not capable of accurately capturing the range of permittivity values relevant for snowpack evolution. A promising next step would be to use a temporally-resolved TDR signal, in which the emission and reception of the electromagnetic wave can be tracked over time. This setup is likely to be more precise, but require the use of more complex equipment and to analyze the temporally-resolved TDR signal. For instance, after discussion, Campbell Scientific suggested the use the TDR200 sensor, and offered to lend us the sensor for a duration of 3 months for further testing.

Another direction for improvement concerns the spike size. The CS655 was initially chosen for this study due to its short spike, which minimizes the impact of snow densification on the sensor's physical integrity. However, the spike length determines the waveguide length, which in turn constrains the time of flight of the signal. In low-permittivity media like snow, this time of flight becomes very short, and may fall below the sensor's capacity. Using a longer spike could increase the time of flight and potentially allow for more accurate measurement of low permittivity. For instance, the CS650 TDR sensor offers a 30cm-long waveguide.

Finally, the experiment described above could be repeated using another material than snow. Indeed, given the difficulties associated with the handling snow and setting up repeatable conditions, using oils with known dielectric properties, and in the same range as snow, could provide a more robust experimental framework. This would removes the uncertainties caused by the probes' insertion, to leave out the sensor-specific uncertainties only.

2 Designing the next field campaign

2.1 Feedbacks of the campaign

This campaign was an opportunity for me to learn how to manage multiple sensors, a knowledge that is important for better planning the next field campaign in 2025/2026 on water percolation in snow that I will coordinate during my PhD at IGE (start in October 2025).

Digging snow pits is a destructive observation method and two different snow pits cannot be dug at the same position. This proved a difficulty at the FluxAlp measurement site, as the field dedicated to snow pits was on non-flat terrain. As a result, the differences in snow depth observed over time are not solely due to melting, but also to variations in the initial snow accumulation. This made comparisons between measurement days difficult.

Probe insertion for WISe or ASSSAP remains the principal source of error. It is difficult to perform multiple measurements with ASSSAP because it is time-consuming. However, WISe is easy to repeat. At the end of the campaign, three measurements along the same eyeline were taken. This seems to be more representative, as it helps eliminate both insertion errors and account for spatial variability in the LWC.

An additional temperature measurement for each snow pit also seems to be a good way to localize the presence of liquid water. PT100 sensors only represent one location near the snow pit, but not within the snow pit itself. Finally, temperature measurements are not time-consuming and can provide valuable information.

The impact of liquid water on SSA is important to analyse. Our study uses a raw stratigraphy which is not located at the same snow pit as the ASSSAP profile drilling. As a result, the stratigraphy does not perfectly match the ASSSAP profile due to differences in snow height and potentially in local stratigraphy. The next step is to colocate the stratigraphy and the ASSSAP profile in order to ensure the reliability of this study's conclusions. Furthermore, this study lacks information on the dry snowpack prior to melting, which is necessary to determine the origin of the capillary barrier.

2.2 Next steps to enhance wet snow investigations on the field

The first prospective goal is to establish a fixed protocol for each snow pit. Our experience during the exploratory 2025 campaign will enable us to define an experimental protocol that is essential for comparing data from day to day, and for building a comprehensive database on wet snow that is consistent in time. This experimental protocol will include systematic measurements of density, SSA, LWC, temperature at same depths, and

stratigraphy.

Secondly, this experimental protocol will be deployed across a range of snow conditions to capture the diversity of snowpack environments. Greenland provides a valuable setting, offering a wide spectrum of snow and climate regimes characteristic of a perennial snowpack. These include the percolation zone (where meltwater percolates into the snowpack down to several meters deep), the wet snow zone (which experiences at least one melt event per year), and with varying melt-to-accumulation ratios and accumulation ratios, already been documented in several studies (Verjans *et al.*, 2019; Samimi *et al.*, 2021). This region is particularly relevant due to its large amount of available cold energy: liquid water can refreeze and sometimes form ice slabs of several meters in thickness. In contrast, coastal Antarctica, such as near the Dumont d'Urville station in Adélie Land, offers very different but complementary conditions. There, melt rates are lower and percolation depths shallower, yet the snowpack dynamics are representative of the early stages of melt. Moreover, these conditions are characteristic of a much broader area than the current Antarctic melting zone, making them critical for understanding its potential future expansion in a warming climate.

The presence of liquid water at the surface influences spectral albedo at specific wavelengths (Dumont *et al.*, 2017). During the campaign, several measurements of spectral albedo, surface liquid water content (LWC, measured using the WISe sensor), and specific surface area (SSA) were conducted simultaneously and at co-located points in wet snow conditions. Although time constraints prevented a full analysis of these datasets, a key next step will be to explore the relationship between spectral albedo and LWC in greater detail.

3 Retrospective and future directions in the development of water percolation schemes

3.1 Analyzing the settings simulations used

For simulations starting during the snow season, the initialization of the snowpack appears to be critical, notably for the representation of capillary barriers and ice crusts. While the simulations that I run for this internship were initialized based on the continuous profiles observed within the snow pits, it could benefit from a better identification of refreezing crusts and SSA contrasts. However, this requires layer matching between the ASSAP and the snow pit profiles.

During this internship I used the standard parametrizations for the BKT (where the water holding capacity must be parametrized) and the RCH (where the water retention curve must be parametrized) schemes. Because the accuracy of water percolation modeling strongly depends on these parameter choices, a sensitivity analysis will be

conducted to assess their influence under different environmental conditions and better understand the strengths and limitations of the schemes themselves, and more generally our ability to model wet snow. This analysis will cover a range of snowpack types, including the French Alps (FluxAlp site), the percolation zone in Greenland ([Samimi *et al.*, 2021](#)), and the coastal regions of Antarctica ([Arioli *et al.*, 2022](#)), and will follow the methodology proposed by [Verjans *et al.* \(2019\)](#).

The added complexity of RCH merits discussion. Richards' equation is crucial to properly represent liquid water movement in soil studies, where pressure head is a critical parameter for plant water uptake and capillary rise in clay-rich soils. In snowpack modeling, computing such a variable is however not as essential. The primary theoretical advantage of RCH lies in its ability to represent capillary barriers. To better assess RCH capability in this regard, idealized or synthetic simulations could be designed to isolate and evaluate its representation of capillary barriers in snow. For instance, the simulation could be driven by a surface energy budget that maintains the snowpack temperature at the melting point, while liquid water is introduced as the top in the form of rainwater. Different idealized snowpacks could be used to study the interactions between layers with prescribed varying SSA and density contrasts. Finally, this simulation setup could also be used to investigate how the presence of a refreezing crust impacts water percolation in the RCH scheme.

3.2 Considerations on the future development of percolation schemes

The sequential treatment of percolation and phase changes leads to major differences between RCH and BKT. This difference is not merely numerical but also rooted in physical dynamics. The key question is: which of these two processes occurs more rapidly in a snowpack? From a microscopic (grain-scale) perspective, one might intuitively argue that heat exchange is the faster dynamic. However, from a macroscopic perspective (considering the percolation of water into the snow matrix and the role of preferential flow paths) it is not obvious which process dominates in speed. This remains an open question. Laboratory experiments could help resolve it by controlling the melting process and precisely measuring temperature profiles throughout the snowpack. Such experiments may provide deeper insight into the coupling between heat and mass transfer in snow under melting and refreezing conditions.

This internship also confirmed a common limitation shared by both the RCH and BKT implementations: the absence of preferential flows, which is a significant component of percolation and likely important to create deep refreezing crusts. The use of a two-domain percolation scheme appears crucial to finely represent the dynamics of percolation. However, the use of a very-high complexity two-domain model (as in [Wever *et al.*, 2016](#)) might be prohibitive for snowpack models that need to maintain a low computational cost. Therefore, part of my future work will be to investigate the use of a percolation scheme of intermediate complexity that can represent the major processes

involved in water percolation, while keeping the computational cost lower than that required to solve the full non-linear system of equations. To that end, I will explore the so-called "invasion-percolation-percolation" models that are used in rock models as a cheaper alternative to Richards' equation ([Cancès et Maltese, 2021](#)).

This study also did not explore in depth the role of refreezing crusts and how they affect percolation in snowpack. A future direction could be to study the interaction between water and these crusts, as well as their representation in snow models, and quantify their implications in terms of mass loss through meltwater runoff.

Conclusion

A set of instruments was deployed at the FluxAlp site (Col du Lautaret, French Alps) to measure the physical properties of the snowpack during the melt period, with a particular focus on its liquid water content. Simulations were conducted at this study site using the Crocus model, and the model sensitivity to two different representations of water percolation, namely the Bucket and Richards schemes, was evaluated. Regarding the in situ characterization of liquid water, obtaining continuous and quantitative measurements remains a significant challenge. While continuous temperature profiles allow us to assess the presence of liquid water, it cannot be used to quantitatively measure the amount of liquid water. While the CS655 TDR sensors, routinely used to measure LWC in soils, seem promising to perform autonomous measurements, they did allow us to measure LWC in snow. Finally, snow pit profiles of LWC using the WISe sensor remain the most robust quantitative method. Nevertheless, only few profiles can be measured. This lack of continuous monitoring doesn't allow a full observation and understanding of the percolation processes.

Qualitative comparison between numerical simulations and the field observations at Col du Lautaret allowed us to identify three mechanisms poorly or not represented in simulations. The first one is capillary barriers: refreezing crusts were clearly present each time a snow pit was dug, indicating local water retention. However, I was not able to produce clear percolation barriers in my simulations, even with the use of Richards equation. Then, after a refreezing crust forms, water destroys the capillary barriers through wet metamorphism: it is then the refreezing crust itself that controls subsequent percolation and water retention. Finally, the observation of warm spots deep below the surface clearly indicates the major role of preferential flow: liquid water seems to flow along "chimneys," allowing it to warm up the bottom of the snowpack, traversing cold portions of the snowpack without refreezing.

Representation of these phenomena was difficult even with a complex scheme like the Richards percolation scheme. This study does not highlight any clear added value of Richards compared to the Bucket scheme at this stage. This questions the real interest of a dynamical resolution of liquid water percolation into snow. Moreover, this work showed that due to different handling of phase changes after (rather than during) the percolation step, Richards melts the lower part of the snowpack, resulting in an earlier melt overall compared to the Bucket scheme, where layers only melt from top to bottom. More than a simple numerical choice, the coupling of liquid water refreezing with percolation highlights the importance of clearly defining the relative speed of the phase change and refreezing processes. Additional research is thus needed to determine which process (refreezing or percolation) is faster under given conditions. This could be achieved with methods of continuous measurement of LWC in snow.

Upcoming research is needed to identify whether density or specific surface area can lead to capillary barrier formation. This may lead to a better understanding of how refreezing crusts develop, which should then be more accurately represented in simulations. Improving percolation schemes by explicitly including capillary barriers and refreezing crusts appears a promising route to enhance the representation of liquid water in natural snowpacks. To that end, a crucial step will be to represent preferential flow to accurately capture the complexity of liquid water percolation.

Bibliography

- AMORY, C., BUIZERT, C., BUZZARD, S., CASE, E., CLERX, N., CULBERG, R., DATTA, R. T., DEY, R., DREWS, R., DUNMIRE, D., EAYRS, C., HANSEN, N., HUMBERT, A., KAITHERI, A., KEEGAN, K., KUIPERS MUNNEKE, P., LENAERTS, J. T. M., LHERMITTE, S., MAIR, D., MCDOWELL, I., MEJIA, J., MEYER, C. R., MORRIS, E., MOSER, D., ORASCHEWSKI, F. M., PEARCE, E., de RODA HUSMAN, S., SCHLEGEL, N.-J., SCHULTZ, T., SIMONSEN, S. B., STEVENS, C. M., THOMAS, E. R., THOMPSON-MUNSON, M., WEVER, N., WOUTERS, B. et THE FIRN SYMPOSIUM TEAM (2024). Firn on ice sheets. *Nature Reviews Earth & Environment*, 5(2):79–99.
- ARIOLI, S., PICARD, G., ARNAUD, L., FAVIER, V. et VANDECURUX, B. (2022). An autonomous multi-band albedometer for long-term monitoring and calibration of optical satellites.
- ARNAUD, L., PICARD, G., CHAMPOLLION, N., DOMINE, F., GALLET, J., LEFEBVRE, E., FILY, M. et BARNOLA, J. (2011). Measurement of vertical profiles of snow specific surface area with a 1 cm resolution using infrared reflectance: instrument description and validation. *Journal of Glaciology*, 57(201):17–29. Publisher: International Glaciological Society.
- BIRCHAK, J., GARDNER, C., HIPPE, J. et VICTOR, J. (1974). High dielectric constant microwave probes for sensing soil moisture. *Proceedings of the IEEE*, 62(1):93–98. Publisher: Institute of Electrical and Electronics Engineers (IEEE).
- BORMANN, K. J., BROWN, R. D., DERKSEN, C. et PAINTER, T. H. (2018). Estimating snow-cover trends from space. *Nature Climate Change*, 8(11):924–928.
- BRUN, E., VIONNET, V., BOONE, A., DECHARME, B., PEINGS, Y., VALETTE, R., KARBOU, F. et MORIN, S. (2013). Simulation of Northern Eurasian Local Snow Depth, Mass, and Density Using a Detailed Snowpack Model and Meteorological Reanalyses. *Journal of Hydrometeorology*, 14(1):203–219.
- CALONNE, N., GEINDREAU, C., FLIN, F., MORIN, S., LESAFFRE, B., Rolland du ROSCOAT, S. et CHARRIER, P. (2012). 3-D image-based numerical computations of snow permeability: links to specific surface area, density, and microstructural anisotropy. *The Cryosphere*, 6(5):939–951.
- CANCÈS, C. et MALTESE, D. (2021). A Gravity Current Model with Capillary Trapping for Oil Migration in Multilayer Geological Basins. *SIAM Journal on Applied Mathematics*, 81(2):454–484. _eprint: <https://doi.org/10.1137/19M1284233>.
- CLERX, N., MACHGUTH, H., TEDSTONE, A., JULLIEN, N., WEVER, N., WEINGARTNER, R. et ROESSLER, O. (2022). In situ measurements of meltwater flow through snow and firn in the accumulation zone of the SW Greenland Ice Sheet. *The Cryosphere*, 16(10):4379–4401. Publisher: Copernicus GmbH.

- D'AMBOISE, C. J. L., MÜLLER, K., OXARANGO, L., MORIN, S. et SCHULER, T. V. (2017). Implementation of a physically based water percolation routine in the Crocus/-SURFEX (V7.3) snowpack model. *Geoscientific Model Development*, 10(9):3547–3566.
- DENOTH, A. (1989). Snow dielectric measurements. *Advances in Space Research*, 9(1): 233–243. Publisher: Elsevier BV.
- DUMONT, M., ARNAUD, L., PICARD, G., LIBOIS, Q., LEJEUNE, Y., NABAT, P., VOISIN, D. et MORIN, S. (2017). In situ continuous visible and near-infrared spectroscopy of an alpine snowpack. *The Cryosphere*, 11(3):1091–1110.
- FOURTEAU, K., BRONDEX, J., CANCÈS, C. et DUMONT, M. (2025). Numerical strategies for representing Richards' equation and its couplings in snowpack models.
- HEILIG, A., EISEN, O., MACFERRIN, M., TEDESCO, M. et FETTWEIS, X. (2018). Seasonal monitoring of melt and accumulation within the deep percolation zone of the Greenland Ice Sheet and comparison with simulations of regional climate modeling. *The Cryosphere*, 12(6):1851–1866.
- KOCHENDORFER, J., NITU, R., WOLFF, M., MEKIS, E., RASMUSSEN, R., BAKER, B., EARLE, M. E., REVERDIN, A., WONG, K., SMITH, C. D., YANG, D., ROULET, Y.-A., BUISAN, S., LAINE, T., LEE, G., ACEITUNO, J. L. C., ALASTRUÉ, J., ISAKSEN, K., MEYERS, T., BRÆKKAN, R., LANDOLT, S., JACHCIK, A. et POIKONEN, A. (2017). Analysis of single-Alter-shielded and unshielded measurements of mixed and solid precipitation from WMO-SPICE. *Hydrology and Earth System Sciences*, 21(7):3525–3542.
- MADORE, J.-B., FIERZ, C. et LANGLOIS, A. (2022). Investigation into percolation and liquid water content in a multi-layered snow model for wet snow instabilities in Glacier National Park, Canada. *Frontiers in Earth Science*, 10:898980.
- PRIESTLEY, A., KULESSA, B., ESSERY, R., LEJEUNE, Y., LE GAC, E. et BLACKFORD, J. (2022). Towards the development of an automated electrical self-potential sensor of melt and rainwater flow in snow. *Journal of Glaciology*, 68(270):720–732. Publisher: Cambridge University Press (CUP).
- QUÉNO, L., FIERZ, C., VAN HERWIJNEN, A., LONGRIDGE, D. et WEVER, N. (2020). Deep ice layer formation in an alpine snowpack: monitoring and modeling. *The Cryosphere*, 14(10):3449–3464. Publisher: Copernicus GmbH.
- RICHARDS, L. A. (1931). CAPILLARY CONDUCTION OF LIQUIDS THROUGH POROUS MEDIUMS. *Physics*, 1(5):318–333. _eprint: https://pubs.aip.org/aip/jap/article-pdf/1/5/318/19666353/1_1745010.pdf.

- ROYER, A., PICARD, G., VARGEL, C., LANGLOIS, A., GOUTTEVIN, I. et DUMONT, M. (2021). Improved Simulation of Arctic Circumpolar Land Area Snow Properties and Soil Temperatures. *Frontiers in Earth Science*, 9:685140.
- SAMIMI, S., MARSHALL, S. J., VANDECRUX, B. et MACFERRIN, M. (2021). Time-Domain Reflectometry Measurements and Modeling of Firn Meltwater Infiltration at DYE-2, Greenland. *Journal of Geophysical Research: Earth Surface*, 126(10): e2021JF006295.
- SAUTER, T., ARNDT, A. et SCHNEIDER, C. (2020). COSIPY v1.3 – an open-source coupled snowpack and ice surface energy and mass balance model. *Geoscientific Model Development*, 13(11):5645–5662.
- STURM, M. et LISTON, G. E. (2021). Revisiting the Global Seasonal Snow Classification: An Updated Dataset for Earth System Applications. *Journal of Hydrometeorology*.
- VAN GENUCHTEN, M. T. (1980). A Closed-form Equation for Predicting the Hydraulic Conductivity of Unsaturated Soils. *Soil Science Society of America Journal*, 44(5):892–898.
- VERJANS, V., LEESON, A. A., STEVENS, C. M., MACFERRIN, M., NOËL, B. et VAN DEN BROEKE, M. R. (2019). Development of physically based liquid water schemes for Greenland firn-densification models. *The Cryosphere*, 13(7):1819–1842.
- VIONNET, V., BRUN, E., MORIN, S., BOONE, A., FAROUX, S., MOIGNE, P. L. et MARTIN, E. (2012). The detailed snowpack scheme Crocus and its implementation in. *Geosci. Model Dev.*
- VIONNET, V., SIX, D., AUGER, L., DUMONT, M., LAFAYSSÉ, M., QUÉNO, L., RÉVEILLET, M., DOMBROWSKI-ETCHEVERS, I., THIBERT, E. et VINCENT, C. (2019). Sub-kilometer Precipitation Datasets for Snowpack and Glacier Modeling in Alpine Terrain. *Frontiers in Earth Science*, 7:182.
- VIVIROLI, D., DÜRR, H. H., MESSERLI, B., MEYBECK, M. et WEINGARTNER, R. (2007). Mountains of the world, water towers for humanity: Typology, mapping, and global significance. *Water Resources Research*, 43(7):2006WR005653.
- WEVER, N., SCHMID, L., HEILIG, A., EISEN, O., FIERZ, C. et LEHNING, M. (2015). Verification of the multi-layer SNOWPACK model with different water transport schemes. *The Cryosphere*, 9(6):2271–2293.
- WEVER, N., WÜRZER, S., FIERZ, C. et LEHNING, M. (2016). Simulating ice layer formation under the presence of preferential flow in layered snowpacks. *The Cryosphere*, 10(6):2731–2744.
- YAMAGUCHI, S., WATANABE, K., KATSUSHIMA, T., SATO, A. et KUMAKURA, T. (2012). Dependence of the water retention curve of snow on snow characteristics. *Annals of Glaciology*, 53(61):6–12.

Appendix A

Method for forcing files creation

1 Gap filling

Forcing data are provided by the meteorological station FLUX-ALPES. They contain a complete dataset covering the 2024-2025 season. Nevertheless, some gaps are present in the dataset, mainly due to sensor malfunctions. The main method developed by Sarah Vermaut used to fill missing data (except for precipitation) was linear interpolation, applied when gaps were shorter than 6 hours. This year was relatively stable, and no gaps longer than 6 hours were detected.

2 Precipitation treatment

The main difficulty concerned the treatment of precipitation data. The sensor does not distinguish between solid and liquid precipitation, and wind-induced under-catch issues affect accuracy. Indeed, observing precipitation is particularly challenging under windy conditions. The stronger the wind, the lower the accuracy of the sensor. This effect is further amplified when precipitation is solid (e.g., snow), requiring a correction function based on wind speed and temperature. In addition, data gaps—combined with the short timescale variability of precipitation (e.g., snowfall occurring over just a few hours)—mean that simple linear interpolation may miss significant events. Again, Sarah Vermaut’s methods were applied to gap-fill the precipitation data.

The first step was to separate solid and liquid precipitation. A commonly used threshold of 1°C was adopted for rainfall–snowfall separation. Then, wind-effect was taken into account with a correction function from [Kochendorfer *et al.* \(2017\)](#), shown in Equation A.1. It was applied to the single-Alter-shielded measurements.

$$CE = e^{-a.U.(1-\arctan(b.T)+c)} \quad (\text{A.1})$$

With: $a = 0.0348$, $b = 1.366$, $c = 0.779$ U : Wind speed [m/s], T : Temperature [K]

The second step was to fill in the gaps in precipitation data. For each gap, visual checks using a webcam at Col du Lautaret, combined with snow depth sensor data, allowed identification of precipitation events. The difference in snow depth measured by the SnowVue (snow height sensor) was interpreted as the total precipitation during the event. To reconstruct the amount of precipitation, the density of fresh snow was estimated using an implemented Crocus formula from [Vionnet *et al.* \(2012\)](#) (Equation A.3). Temperature and wind speed were averaged over the duration of the event, and the calculated precipitation (Equation A.2) was distributed uniformly over the event period.

$$Q = Z \cdot \frac{\rho_{snow}}{\rho_e} \quad (\text{A.2})$$

With: ρ_{snow} : fresh snow density, ρ_e : water density, Z : snow depth difference between the beginning and the end of the snow event.

$$\rho_{s-new} = a_\rho + b_\rho(T_a - T_{fus}) + c_\rho \cdot U^{1/2} \quad (\text{A.3})$$

With: $a_\rho = 109 \text{ kg} \cdot \text{m}^{-3}$, $b_\rho = 6 \text{ kg} \cdot \text{m}^{-3} \cdot \text{K}^{-1}$, and $c_\rho = 26 \text{ kg} \cdot \text{m}^{-7/2} \cdot \text{s}^{-1/2}$.

Despite these corrections and the gap-filling, a significant difference remains between the observed snow depth and the simulated snow depth using precipitation from the corrected rain gauge data, as shown in Figure A.2. Some snow events appear to be overestimated, such as at the beginning of January, while others seem to be underestimated, particularly throughout February and March. This discrepancy results in an earlier complete melt of the simulated snowpack.

This bias can be potentially explained by the local topography of the FluxAlp station (Figure A.1). First, FluxAlp is located near Col du Lautaret, an area known for strong winds that can blow away freshly fallen snow. Second, the station is situated on the sloped side of a topographic depression, which is inversely oriented to the dominant wind direction. The combination of these two effects can lead to either over-accumulation or under-accumulation of snow, depending on wind conditions during snow events.

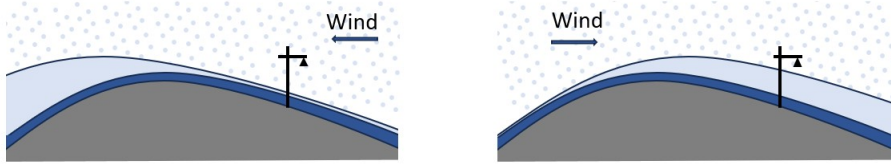


Figure A.1: Schematic of the relative topography of the FluxAlp station to explain over- and under-accumulation snow events.

Because classic precipitation corrections do not match the observed snow depth, I explored another method for reconstructing precipitation. The same approach used for gap-filling was applied to the entire 2025 season. An interval-based discretization was used to divide the season into a temporal grid. Within each interval, the observed snow depth difference was calculated. To reduce the impact of measurement noise, a threshold of 5 cm was applied. When the snow depth change exceeded this threshold, a snow event was identified. The fresh snow density is calculated using Equation A.3, which allows the calculation of the amount of precipitation.

Figure A.2 presents the simulation results using two different time intervals: 3 h and 24 h. The smaller the interval, the more accurately overestimated snowfall events are captured. On the other hand, a larger interval may fail to capture snowfall events with no accumulation due to wind transport and may not consider them as snowfall. The best balance can be found, or problematic snowfall events can be removed from the observed snow depth.

This study aims to accurately reproduce snow events during the melting season (February to April). Among the tested configurations, the Crocus precipitation recon-

struction using a 3 h interval provides the most satisfactory results for this time period. Therefore, this 3 h precipitation reconstruct with Crocus formula, forcing file will be used for the remainder of the study.

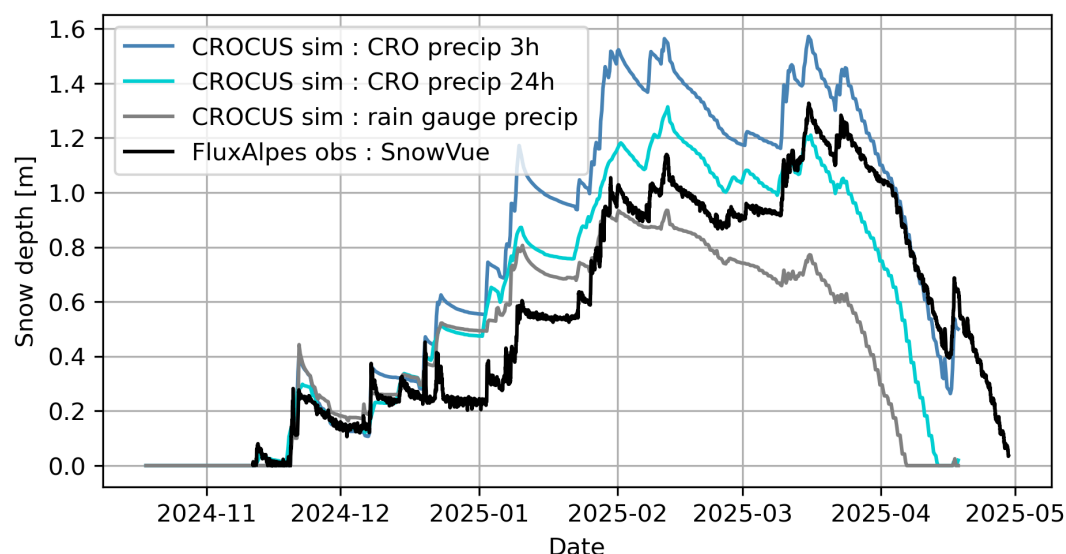


Figure A.2: Observed snow depth (black) at Col du Lautaret from SnowView vs. Crocus-simulated snow depth forced with various precipitation inputs: "Obs precip" uses SnowView-observed precipitation; "CRO precip 3h no Smooth" and "CRO precip 24h no Smooth" use reconstructed precipitation from snow depth using the Crocus density formula over 3h and 24h intervals

Keys Note : *FluxAlp meteorological data were used. To that end, gap filling was performed by interpolation using Sarah Vermaut's method. Particular attention was paid to reproducing precipitation consistent with the observed snow depth throughout the season.*

Appendix B

Detailed description of Bucket and Richards percolation scheme

1 Modelling liquid water percolation in snow: the bucket scheme

Liquid mass transfer was historically developed in Crocus using the bucket approach. This is a straight-forward and numerically efficient numerical scheme, but which relies on a simplified description of percolation and capillary effects in snow.

At the start of the bucket routine, an initial liquid water field is computed based on snow melting and liquid precipitation. Then, each layer is seen as a bucket that can hold a certain amount of water. This holding capacity is defined as a percentage of pore space (5% percent in Crocus). If more water is introduced into the snow layer than it can retain, the water is transferred to the layer below.

With this method, refreezing is managed during percolation at each layer. Water that penetrates a cold layer will refreeze first. Once the cold content is exhausted, the remaining water continues to percolate. Implicitly, this supposes that refreezing occurs faster than percolation. Note that other detailed snow models, such as COSIPY (Sauter *et al.*, 2020), make the opposite assumption, allowing all the water to percolate first and then refreezing it afterward. Finally, when the water reaches the bottom of the snowpack, it is considered like runoff and is managed by another component of SURFEX.

2 Modelling liquid water percolation in snow: Richards equations

Richards' percolation scheme is based on Richards' equation (Richards, 1931), and has been initially implemented in Crocus (D'Amboise *et al.*, 2017). For this internship, I use a more recent implementation, based on the study of Fourteau *et al.* (2025).

While originally developed for soils, this model should in principle more faithfully represent liquid water percolation, capturing the complexity of percolation and better reflecting the role of capillary forces on water movement through snow. Richards' equation is based on liquid water mass conservation, in which the liquid water flux follows Darcy-Buckingham's law (valid for both saturated and unsaturated media) combined with mass conservation. It is a non-linear equation that accounts for the complex dependence of the liquid water flux to the volumetric water content, θ . The liquid water flux F_w is taken as a gradient law:

$$F_w = -K(\theta)\nabla H(\Theta) \quad (\text{B.1})$$

With:

- θ : Volumetric water content (dimensionless)
- $K(\theta)$: Hydraulic conductivity (in m s^{-1})
- $H(\theta) = h - z$: Hydraulic potential define by pressure head h and the altitude z (in m).

Combined with mass conservation, Richards' equation finally reads:

$$\frac{\partial \theta}{\partial t} = \frac{\partial}{\partial z} \left(K(\theta) \cdot \frac{\partial H}{\partial z} \right). \quad (\text{B.2})$$

In Richards' equation, water flows due to water potential difference in order to reach equilibrium. This potential H is related to the volumetric water content θ through the pressure h and a so-called water retention curve $h(\theta)$. For this internship, I used the Van Genuchten law for the water retention curve (Van Genuchten, 1980). This law is parametrized using the fit parameters for snow proposed by Yamaguchi *et al.* (2012). The Van Genuchten model (displayed in Figure B.1) describes how the suction of a porous medium depends on its volumetric water content. When the medium is fully saturated, the suction is zero. Conversely, as the medium dries, the suction capacity increases, reflecting the tendency of dry media to absorb water through capillary forces. In the van Genuchten law, the suction tends to infinity as the medium becomes drier. Physically, such a divergence implies that drying the medium below its retention level would be impossible. In other words, if the standard van Genuchten law were to actually apply in snow, an at least 2% liquid water content would always be present in snow. To allow the existence of dry snow, a cutoff is introduced in the Van Genuchten, seen in the right panel of Figure B.1. This regularization also appears to be beneficial for the numerical cost of numerical models (Fourteau *et al.*, 2025).

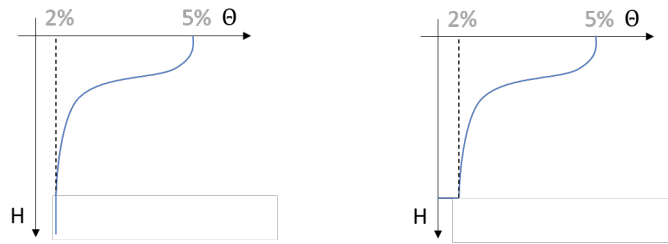


Figure B.1: Schematic Van Genuchten Model With and Without Cutoff (Right/Left)

Hydraulic conductivity is the transport coefficient setting the dynamics (i.e. how fast) of liquid water flow. It is taken as the product of a saturated hydraulic conductivity (depending on only the porous microstructure) and of the relative permeability $k_r(\theta)$, which depends on the volumetric water content:

$$K(\theta) = k_r(\theta) \cdot K_{\text{sat}}(D, \rho_{\text{snow}}). \quad (\text{B.3})$$

In the case of snow, the saturated hydraulic conductivity depends on the (dry) density and on the SSA. This dependence was determined by [Calonne *et al.* \(2012\)](#) through tomography images.

For the relative hydraulic conductivity, we follow the formula of van Genuchten-Mualem [Van Genuchten \(1980\)](#), which uses the same parameters as the van Genuchten law for hydraulic potential [Yamaguchi *et al.* \(2012\)](#).

